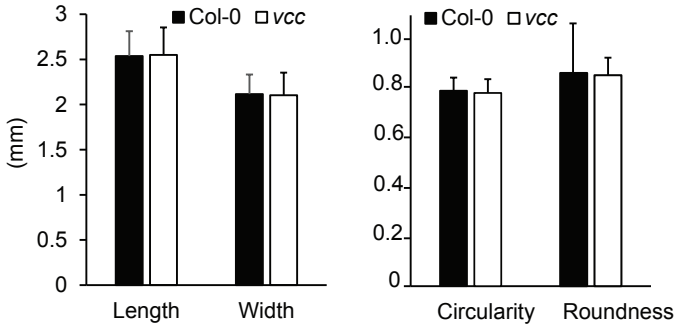

Fig. S1. Size and shape of wild-type and *vcc* cotyledons.(A) Length and width of cotyledons from seedlings of Col-0 and *vcc* at 8 days after germination. Mean + SD (n=100 cotyledons per genotype).
(B) Shape parameters circularity and roundness in wild-type and *vcc* cotyledons; Mean + SD (n = 100 cotyledons per genotype).

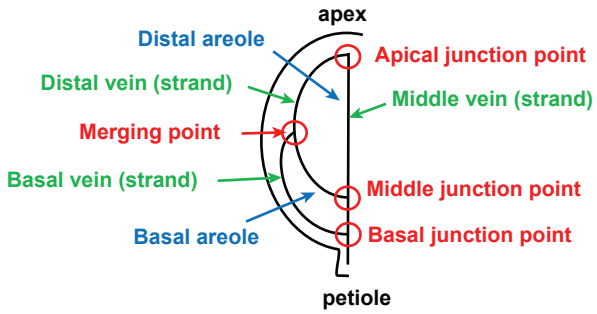

Fig. S2. Terminology to describe geometry of vein pattern in cotyle-dons.
The diagram indicates veins and vein merging points in half of an *Arabidopsis* cotyledon. An areole is the area enclosed by veins. The term “strand” denotes developing veins consisting of pre-procambial/procam-bial cells.

Development • Supplementary information

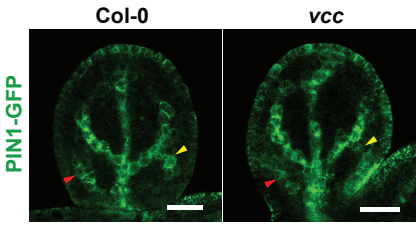

Fig. S3. Basal strand formation in wild type and *vcc* cotyledons. Basal strands originate from the first (yellow) or second (red) PIN1 domains in wild-type and *vcc* cotyledons (approximately 140 µm in length).
Scale bars = 30 µm.

Nucleotide sequence
PID
226 CGCCTCAT GCGTCGTATCGGCGCCGGCGACATCGGAACAGTTTAC 270
pid-17
226 CGCCTCATGGCGTCGTATCGGCGCCGGCGACATCGGAACAGTTTAC 271
pid-18
226 CGCCTCATTGCGTCGTATCGGCGCCGGCGACATCGGAACAGTTTAC 271

Deduced amino acid sequences
PID
76 RLMRRIGAGDIGTVY 90
PID-17
76 RLMASYRRRRHRNSL 90
PID-18
76 RLMASYRRRRHRNSL 90

Fig. S4. Identification of mutations in CRISPR/ CAS9-edited lines.
Nucleotide and deduced amino acid sequences of PID, *pid-17*, and *pid-18*. Under-lined nucleotides show the PAM sequence. Single nucleotide G and T (highlighted by red color) were inserted after the nucleotide 233 from the translation site in *pid-17* and *pid-18*, respectively. Predicted amino acid changes (highlighted in red) in PID-17 and PID-18 mutant proteins.

Development • Supplementary information

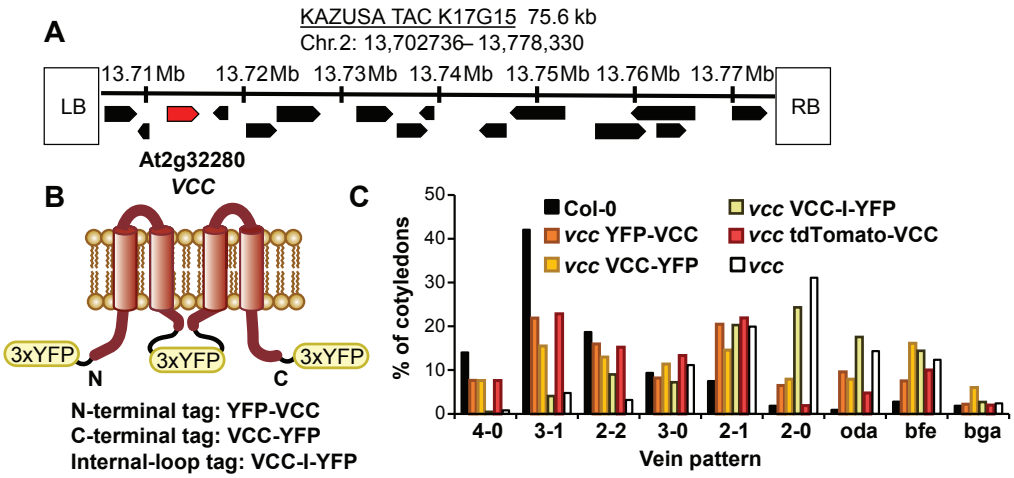

Fig. S5. Fluorescent protein-tagged VCC versions and rescue analysis.
(A) The KAZUSA TAC clone K17G15 contains the *VCC* genomic sequence. (B) Predicted structure of VCC at a membrane and positions of the 3x-YFP tag. (C) Rescue analysis of 3x-YFP- and tdTomato-tagged VCC in the *vcc* mutant back-ground. Average of three independent transgenic lines are shown, except for VCC-I-YFP for which two lines were analyzed.

Development • Supplementary information

Supplementary Table 1: Statistical analyses of vein network complexity and vein disconnections

Chi-squared test: vein network complexity (Fig 5a)		
Comparison	Raw P-value	Adjusted P-value
Col-0 vs En-1	0.2471	0.2745
Col-0 vs *vcc*	0.0001	0.0001
Col-0 vs *pin1-1*	0.0000	0.0001
Col-0 vs *vcc pin1-1*	0.0000	0.0000
En-1 vs *vcc*	0.0043	0.0071
En-1 vs *pin1-1*	0.0032	0.0064
En-1 vs *vcc pin1-1*	0.0000	0.0000
vcc vs *pin1-1*	0.8781	0.8781
vcc vs vcc *pin1-1*	0.0289	0.0414
pin1-1 vs vcc *pin1-1*	0.0541	0.0676

Chi-squared test: connectivity related (Fig 5a)		
Comparison	Raw P-value	Adjusted P-value
Col-0 vs En-1	0.1049	0.1748
Col-0 vs *vcc*	0.0008	0.0038
Col-0 vs *pin1-1*	0.0028	0.0092
Col-0 vs *vcc pin1-1*	0.0000	0.0003
En-1 vs *vcc*	0.0767	0.1533
En-1 vs *pin1-1*	0.1356	0.1938
En-1 vs *vcc pin1-1*	0.0065	0.0162
vcc vs *pin1-1*	0.8665	0.8665
vcc vs vcc *pin1-1*	0.3482	0.3869
pin1-1 vs vcc *pin1-1*	0.2573	0.3216

Chi-squared test: complexity (Fig 5b)		
Comparison	Raw P-value	Adjusted P-value
Col-0 vs *vcc*	0.0000	0.0000
Col-0 vs *pid-14*	0.0000	0.0000
Col-0 vs *pid-17*	0.0000	0.0000
Col-0 vs *vcc pid-18*	0.0000	0.0000
vcc vs *pid-14*	0.4684	0.5855
vcc vs *pid-17*	0.0553	0.1105
vcc vs *vcc pid-18*	0.7509	0.8343
pid-14 vs *pid-17*	0.2265	0.3775
pid-14 vs *vcc pid-18*	1.0000	1
pid-17 vs *vcc pid-18*	0.2992	0.4274

Chi-squared test: connectivity (Fig 5b)		
Comparison	Raw P-value	Adjusted P-value
Col-0 vs *vcc*	0.0001	0.0002
Col-0 vs *pid-14*	0.0000	0.0000
Col-0 vs *pid-17*	0.0044	0.0063
Col-0 vs *vcc pid-18*	0.0000	0.0000
vcc vs *pid-14*	0.6702	0.6702
vcc vs *pid-17*	0.3701	0.4112
vcc vs *vcc pid-18*	0.0000	0.0000
pid-14 vs *pid-17*	0.1442	0.1803
pid-14 vs *vcc pid-18*	0.0000	0.0000
pid-17 vs *vcc pid-18*	0.0000	0.0000

Development • Supplementary information